

## Asymmetric flux pinning in laterally nanostructured ferromagnetic / superconducting bilayers

M. LANGE<sup>1</sup> (\*), M. J. VAN BAEL<sup>1</sup>, L. VAN LOOK<sup>1</sup>, K. TEMST<sup>1</sup>, J. SWERTS<sup>1</sup>, G. GÜNTHERODT<sup>2</sup>, V. V. MOSHCHALOV<sup>1</sup> and Y. BRUYNSERAEDE<sup>1</sup>

<sup>1</sup> *Laboratorium voor Vaste-Stoffysica en Magnetisme, K.U.Leuven - Celestijnenlaan 200D, B-3001 Leuven, Belgium*

<sup>2</sup> *2. Physikalisches Institut, RWTH Aachen - D-52056 Aachen, Germany*

PACS. 74.60.Ge – Flux pinning, flux creep, and flux-line lattice dynamics.

PACS. 74.80.Dm – Superconducting layer structures: superlattices, heterojunctions, and multilayers.

PACS. 75.70.-i – Magnetic films and multilayers.

**Abstract.** – We investigated the pinning of flux lines in a superconducting film by a regular array of *magnetic antidots*. The sample consists of a Co/Pt multilayer with perpendicular magnetic anisotropy in which a regular pattern of submicron holes is introduced and which is covered by a type-II superconducting Pb film. The resulting ferromagnetic/superconducting heterostructure shows a pronounced asymmetric magnetization curve with respect to the field polarity. This asymmetry clearly demonstrates that the magnetic contribution dominates the pinning potential imposed by the magnetic antidots on the superconducting film.

Strong pinning of flux lines (FLs) is a prerequisite for a superconductor to achieve a high critical current density  $j_c$ , a condition that for instance can be realized by artificially introducing regularly distributed pinning centres (*e.g.* antidots) in a superconducting film. The resulting commensurability between the flux line lattice (FLL) and the periodic pinning potential created by the regular array of antidots in the superconductor is clearly observed as peaks or shoulders in the curves of the magnetization  $M(H)$  or  $j_c(H)$  [1–5], with  $H$  the perpendicularly applied magnetic field.

Recently, the interest shifted to the pinning behaviour of submicron *magnetic* pinning arrays in contact with a superconductor [6–14]. In this letter we present an experimental study of the flux pinning in a superconducting Pb film in contact with a Co/Pt multilayer with an array of submicron holes (*magnetic antidots*). The correct choice of preparation conditions and film thicknesses produces a Co/Pt multilayer with perpendicular magnetic anisotropy [15]. Several terms can contribute to the pinning mechanism in this hybrid ferromagnetic/superconducting system, *e.g.*, the corrugated surface of the Pb film due to the deposition on top of the Co/Pt antidot array, the high magnetic permeability of the ferromagnet [6,7], the direction and magnitude of the magnetic moment [9,10], and the local stray field of the ferromagnet [10–12]. We show that the  $M(H)$  curve of the above described heterostructure is strongly asymmetric,

---

(\*) E-Mail: [Martin.Lange@fys.kuleuven.ac.be](mailto:Martin.Lange@fys.kuleuven.ac.be)

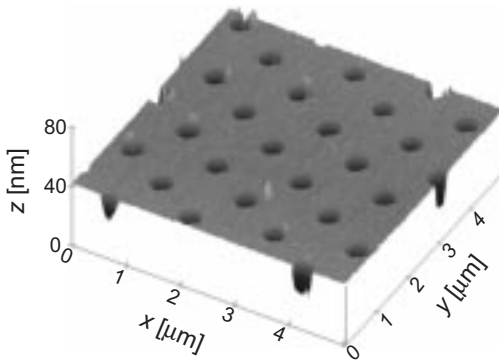


Fig. 1

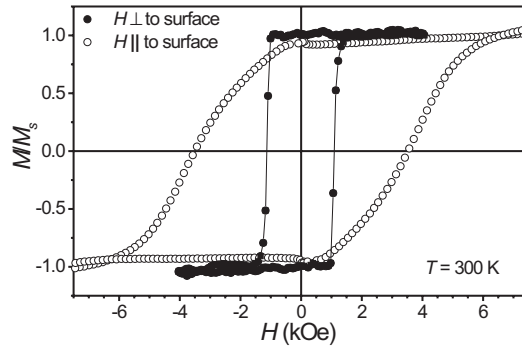


Fig. 2

Fig. 1 – AFM image ( $5 \mu\text{m} \times 5 \mu\text{m}$ ) of the Co/Pt multilayer with a square array of antidots. The antidot array has a period of  $1 \mu\text{m}$  and the side length of an antidot is about  $370 \text{ nm}$ .

Fig. 2 – MOKE hysteresis loops measured at room temperature of the Co/Pt multilayer with antidots obtained with the field  $H$  applied parallel ( $\circ$ ) and perpendicular ( $\bullet$ ) to the surface.

which excludes the corrugated surface of the Pb film as the main origin of the observed matching effects. Hence, the magnetic interaction between FLs and pinning centres dominates the pinning mechanism. The asymmetric  $M(H)$  curves are explained by a model based on the presence of vortices created by the stray field of the magnetic antidots.

We will first describe the sample preparation and the magnetic characterization of the Co/Pt antidot film by means of magneto-optical Kerr effect (MOKE) hysteresis loop and magnetic force microscopy (MFM) measurements. In the second part, we analyse the magnetization data obtained by a SQUID magnetometer.

The square array of magnetic antidots is prepared by evaporating a  $17 \text{ nm}$  thick Co/Pt multilayer in a resist mask on an amorphous  $\text{SiO}_2$  substrate held at room temperature. The resist mask is prepatterned by electron-beam lithography, and after the deposition of the Co/Pt multilayer the resist is removed using a standard lift-off procedure. The patterned area is about  $9 \text{ mm}^2$ . The Co/Pt multilayer is deposited in an MBE system by e-beam evaporation with typical Pt and Co deposition rates of about  $0.06 \text{ nm/s}$ , controlled by a quartz crystal oscillator. The multilayer consists of a  $2.8 \text{ nm}$  Pt base layer to improve the perpendicular anisotropy [16], and a multilayer structure of  $[\text{Co}(0.4 \text{ nm})/\text{Pt}(1.0 \text{ nm})]_{10}$ .

An atomic force microscopy (AFM) measurement of the antidot array is shown in fig. 1 and reveals a well-defined square arrangement of the antidot array with a period of  $1 \mu\text{m}$ . The antidots have a square shape with rounded corners and a side length of about  $370 \text{ nm}$ .

The Co/Pt antidot array is covered with a continuous type-II superconducting Pb film to study the flux pinning properties of the magnetic antidots. In order to prevent the direct influence of the proximity effects between Pb and Co/Pt, a  $10 \text{ nm}$  insulating amorphous Ge layer is deposited first with a growth rate of  $0.2 \text{ nm/s}$ , then the  $50 \text{ nm}$  Pb film is evaporated at a substrate temperature of  $77 \text{ K}$  with a growth rate of  $1.0 \text{ nm/s}$  and finally, the sample is covered with a  $30 \text{ nm}$  Ge layer for protection against oxidation. Note that the Pb layer is significantly thicker than the Co/Pt multilayer, which ensures a complete coverage of the magnetic antidots.

To confirm that the easy axis of magnetization of the Co/Pt multilayer with antidots is per-

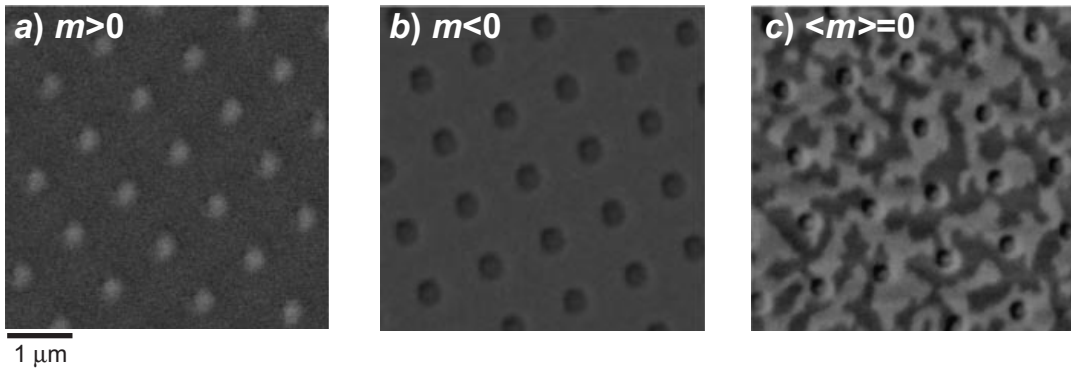


Fig. 3 – MFM images ( $5\ \mu\text{m} \times 5\ \mu\text{m}$ ) measured in  $H = 0$  of the Co/Pt multilayer with antidots *a*) after magnetization in  $H = +10\ \text{kOe}$ , *b*) after magnetization in  $H = -10\ \text{kOe}$  and *c*) after demagnetization.

pendicular to the surface, we measured MOKE hysteresis loops at room temperature in two different field configurations before the patterned multilayer was covered with the Ge/Pb/Ge trilayer (see fig. 2). With the field  $H$  applied perpendicular to the sample plane, the loop has a rectangular shape with a saturation field of  $H_s = 1.5\ \text{kOe}$  and a coercive field of  $H_c = 1.1\ \text{kOe}$ . When  $H$  is applied parallel to the surface, we obtain  $H_c = 3.5\ \text{kOe}$  and  $H_s \approx 7\ \text{kOe}$ . These results indicate that the easy axis of magnetization is perpendicular to the surface. At low temperatures ( $T = 5\ \text{K}$ ), SQUID measurements on a Co/Pt reference multilayer without any patterning show that the 100 % remanent magnetization of the hysteresis loop obtained with  $H$  perpendicular to the surface is preserved, while  $H_c$  is slightly enlarged.

For the interpretation of the flux pinning phenomena in the ferromagnetic/superconducting hybrid structure, it will be important to obtain microscopic information about the domain structure and the related stray field patterns of the Co/Pt antidot array. For that reason we have carried out MFM measurements of the patterned multilayer without Ge/Pb/Ge trilayer using a Digital Instruments Nanoscope III system at room temperature and zero field. The magnetic moment of the tip is pointing perpendicular to the surface, which makes it sensitive to the perpendicular component of the stray field emanating from the surface. The experiments are carried out using the tapping/lift<sup>TM</sup> mode [17] with a typical scan height of 50 – 80 nm above the sample surface. Figure 3 shows three  $5\ \mu\text{m} \times 5\ \mu\text{m}$  MFM scans of the sample in three different magnetic states. The magnetic moments  $\mathbf{m}$  of the Co/Pt multilayer are aligned into different directions before the MFM measurement by applying a field perpendicular to the surface of (fig. 3*a*)  $H = 10\ \text{kOe}$  ( $m = |\mathbf{m}| > 0$ ), and (fig. 3*b*)  $H = -10\ \text{kOe}$  ( $m < 0$ ). In fig. 3*c*, the sample was demagnetized in an out-of-plane field oscillating around zero with decreasing amplitude before the MFM measurement ( $\langle m \rangle = 0$ ). In fig. 3*a*, bright spots are observed at the position of the antidots, which can be explained by the fact that the out-of-plane components of the stray field  $\mathbf{h}$  above the antidots and above the multilayer are oriented in a mutually opposite direction. When  $m < 0$  (fig. 3*b*), the spots appear in a darker colour, corresponding to the other polarity of  $\mathbf{h}$  compared to the  $m > 0$  state. In fig. 3*c*, the bright and dark regions between the antidots can be identified as magnetic domains in the Co/Pt multilayer, where the magnetization is directed either parallel or antiparallel to the tip magnetization. The observed domain structure is typical for thin magnetic films with perpendicular anisotropy (see *e.g.* [18]) and the average domain size amounts to a few 100 nm. The contrast at the edges of the antidots might be due to some tip effects because of the

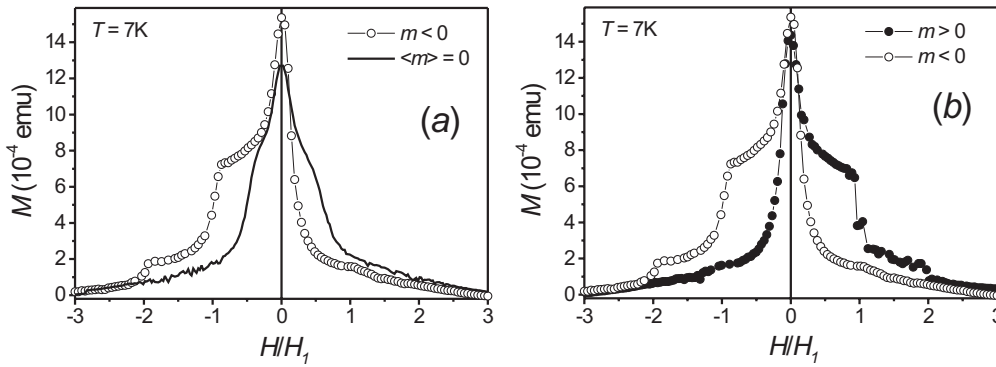


Fig. 4 – SQUID magnetization curves at  $T = 7$  K of a superconducting Pb film on top of a magnetic Co/Pt antidot lattice, with the antidot lattice in different magnetic states: *a*) ( $\circ$ )  $m < 0$  and full line  $\langle m \rangle = 0$ , *b*) ( $\circ$ )  $m < 0$  and ( $\bullet$ )  $m > 0$ .

topography. It is clear that the created stray field pattern in fig. 3c is different from the one that is found when the sample is magnetized (fig. 3a and 3b).

We will now investigate how the different magnetic states of the sample influence the flux pinning phenomena in the superconducting Pb layer. After covering the magnetic antidots with the type-II superconducting Pb film,  $M(H)$  curves have been measured below the critical temperature  $T_c$  of the Pb film in a Quantum Design SQUID magnetometer with  $H$  perpendicular to the film plane. From  $M(T)$  measurements we determined  $T_c = 7.20$  K. Figure 4 shows the upper branches ( $M > 0$ ) of the  $M(H)$  loops of the sample at  $T = 7$  K. The lower branches ( $M < 0$ ) are mirror images of the upper branches with respect to the field axis. The field scale is normalized to the first matching field  $H_1 = \phi_0 / (1 \mu\text{m})^2 = 20.67$  Oe, at which  $H$  generates exactly one flux quantum  $\phi_0$  per unit cell of the magnetic antidot array [2–5].  $H$  is always much smaller than the coercive field  $H_c$  of the Co/Pt multilayer with antidots, so that the magnetic state of the multilayer remains unchanged for each of the displayed curves in fig. 4. The ferromagnetic contribution of the Co/Pt multilayer to the total magnetization  $M$  results in an offset of the order of  $\sim 10^{-5}$  emu depending on its magnetic state. The preservation of the magnetic state is confirmed by an unchanged offset after measuring the  $M(H)$  curves.

It is clear from fig. 4a that the  $M(H)$  curve for  $m < 0$  is *strongly asymmetric* with respect to the polarity of the applied field, very similar to what was observed recently for a superconducting film on top of a lattice of magnetic dots with out-of-plane magnetization [9, 10]. For the  $m < 0$  state, the magnetization  $M$  has a larger value at negative fields than at the corresponding positive fields, indicating a much stronger flux pinning when  $H$  and  $m < 0$  are pointing in the same direction. The field polarity dependent pinning strength can also be noticed in the matching effects, which appear at integer negative matching fields at  $H/H_1 = -1$  and  $-2$ , while for their positive counterparts, only a small deviation from the smooth curve is visible at  $H/H_1 = 1$ . No matching effect can be seen at  $H/H_1 = 2$ . In the  $\langle m \rangle = 0$  state, a symmetric  $M(H)$  curve is obtained (solid line in fig. 4a), with only weak matching effects appearing as shoulders at  $H/H_1 = +1/2$  and  $-1/2$ . Figure 4b illustrates that the asymmetry of the  $M(H)$  curves is *reversed* when  $m > 0$ . The enhanced matching effects and the larger value of  $M$  now appear at positive fields.

Figure 5 shows the temperature dependence of the  $M(H)$  curves with the magnetic antidots in

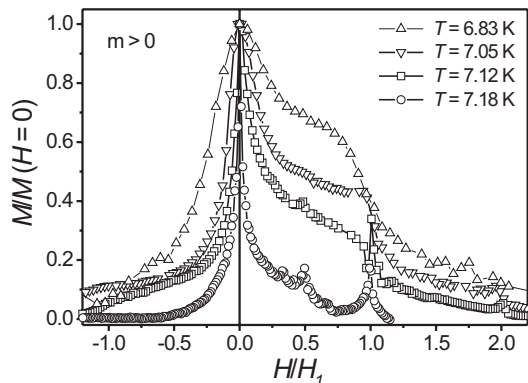


Fig. 5

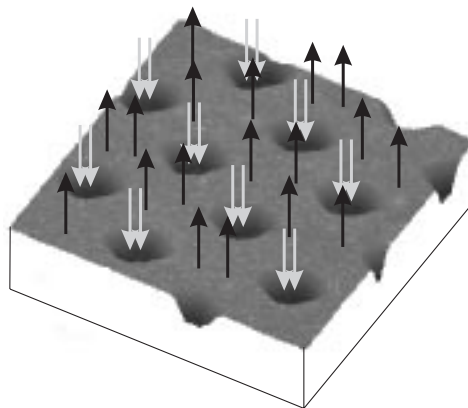


Fig. 6

Fig. 5 – Magnetization curves of a superconducting Pb film on top of a Co/Pt antidot lattice ( $m > 0$ ) at different temperatures: ( $\Delta$ )  $T = 6.83$  K, ( $\nabla$ )  $T = 7.05$  K, ( $\square$ )  $T = 7.12$  K and ( $\circ$ )  $T = 7.18$  K.

Fig. 6 – Schematic drawing to illustrate the proposed model for  $m > 0$  and  $H = 0$ : vortices (black arrows) and antivortices (grey arrows) are induced in the superconductor by the stray field of the patterned Co/Pt multilayer. The value of the stray field corresponds to  $2\phi_0$  per unit cell of the antidot array. The antivortices act as a regular array of pinning centers for external flux lines.

the  $m > 0$  state. At temperatures close to  $T_c$ , we observe additional rational matching effects at positive fields ( $H/H_1 = 1/3, 1/2$  and  $2/3$  at  $T = 7.18$  K, and  $H/H_1 = 1/2$  at  $T = 7.12$  K), no matching effects can be seen at negative fields. If the temperature is decreased, the rational matching effects disappear and the integer matching effects are smeared out ( $T = 6.83$  K). This is also observed in thin superconducting films with lattices of antidots [2]. However, the  $M(H)$  curve keeps its asymmetry down to the lowest measured temperature of 5 K.

The  $M(H)$  data show that vortices are much stronger pinned when  $H$  and  $m$  have the same polarity. This observation raises the question: which contributions to the pinning potential are responsible for the asymmetry?

The *surface modulation* of the Pb film cannot explain the asymmetry of the  $M(H)$  curves, since its contribution to the pinning potential is not depending on the direction of  $H$ . For the same reason, the high *magnetic permeability* of the ferromagnetic material can not be the origin of the asymmetry. For magnetic dots with perpendicular anisotropy as pinning centres, the asymmetric behaviour has been related to the interaction between the magnetic moments  $\mathbf{m}$  of the magnetic dots and the applied field  $\mathbf{H}$ , in terms of a *magnetic interaction energy*  $E = -\mathbf{m} \cdot \mathbf{H}$  [9, 10]. Evaluating this term for the magnetic antidots, the clearest matching effects should appear when  $H$  and  $m$  have opposite polarity (in this case FLs are forced into the position of the antidots, which are acting as sharply defined pinning centers). This is in contrast to what is observed in this experiment, therefore the term  $E = -\mathbf{m} \cdot \mathbf{H}$  cannot dominate the pinning potential.

Recent vortex imaging experiments investigating in-plane magnetized dots in contact with a superconductor have shown that the stray field of the dots can induce vortex-like structures in the superconductor. These induced vortices play a crucial role in the flux pinning properties of the dots [12]. Also for magnetic dots with out-of-plane magnetization, the existence of induced vortices has been predicted by theory [13, 14, 19]. Magnetic antidots have the inverse

geometry of magnetic dots, therefore the stray fields of dots and antidots are very similar to each other. We will now show that the asymmetric  $M(H)$  curves in fig. 4 can be explained by the presence of such stray field induced vortices in the superconductor.

Based on the above considerations for magnetic dots, we propose the following model when magnetic antidots are used as pinning centers: The presence of the stray field will create supercurrents in the superconductor. In order to estimate the magnitude of the stray field, we have carried out magnetostatical calculations (based on the theory in [20]) for magnetic antidots with the same geometry and magnetization as in this experiment. At a height of 35 nm above the surface of the Co/Pt multilayer, the amount of flux that is created by the ferromagnet corresponds to about  $2 \times \phi_0$  ( $\phi_0$  is the flux quantum) in each unit cell of the magnetic antidot array. Hence, it appears reasonable to assume that the local stray fields cannot be completely shielded by the Meissner currents and at least one vortex per unit cell of the magnetic antidot array is created by the stray field. It is possible that different unit cells contain different amounts of flux quanta, *e.g.* when the average created flux in one unit cell above the ferromagnet is  $r \times \phi_0$ , with  $r$  a non-integer number.

In the  $m > 0$  state, we assume that these induced vortices with a local magnetic field  $h > 0$  will be located at the interstitial positions of the antidot array (see black arrows in fig. 6). Since stray field emanating from the Co/Pt multilayer must return somewhere, antivortices with  $h < 0$  will appear at the position of the antidots (grey arrows in fig. 6). The existence of vortex-antivortex pairs induced by stray field is also predicted in the case of magnetic dots with out-of-plane magnetization [13, 14]. Vortices and antivortices can not annihilate, since the vortices must be located at the interstitial positions, whereas the antivortices are fixed at the antidots. The number of antivortices and vortices in the superconductor in zero field must be the same (neglecting effects at the sample boundary).

We will now discuss how the behaviour of the system in an applied magnetic field can be described by means of the above model. To avoid any confusion concerning the use of the terms *vortex*, *antivortex* and *FL*, we will always use the terms *vortices* and *antivortices* when they are induced by the magnetic Co/Pt multilayer (vortices located at the interstices and antivortices at the antidots) and *FLs* when they are created by an externally applied field. When  $H \neq 0$  is applied, the additional FLs will interact with the vortices and antivortices. If FLs and vortices have the same field polarity, they have a repulsive interaction, while FLs and vortices with opposite field polarity attract each other. The antivortices are fixed at the position of the antidots and therefore form a strongly regular pinning potential for the FLL, with a period corresponding to the period of the antidot array. The vortices at the interstitial positions are more mobile and do not form such a regular array, see fig. 6.

When  $H > 0$  and  $m > 0$ , FLs and antivortices have an attractive interaction and therefore, matching effects and an enhanced value of  $M$  are observed. When  $H < 0$  and  $m > 0$ , FLs and antivortices have the same polarity and repel each other, so that the FLs are forced into the interstitial positions. Hence, a lower value of  $M$  and only weak matching effects are observed compared to the case when  $H > 0$  and  $m > 0$ . This model also explains the reversal of the asymmetry when the film is magnetized in the opposite direction ( $m < 0$ ). The almost symmetric  $M(H)$  curve obtained for demagnetized magnetic antidots ( $\langle m \rangle = 0$ ) can be explained by the absence of an asymmetric pinning potential. Due to the domain structure (see fig. 3c), antivortices can also appear at the interstitial positions. However, the weak matching effects at  $H/H_1 = +1/2$  and  $-1/2$  indicate that the pinning potential still has a certain periodicity, *e.g.*, due to non-magnetic contributions such as the surface modulation of the Pb.

In conclusion, a lattice of antidots in a magnetic film with perpendicular anisotropy creates a strong pinning potential for flux lines in a type-II superconductor. Pronounced asymmetric  $M(H)$  curves are observed, indicating significantly enhanced pinning when  $m$  and  $H$  are

parallel. To explain this asymmetry, a qualitative model is proposed which is based on the presence of vortices and antivortices induced by the stray field of the magnetic antidots. A quantitative theoretical treatment and further experiments by local vortex imaging techniques are needed to confirm this model.

\* \* \*

The authors would like to thank R. Jonckheere for the preparation of the resist pattern and U. May, P. Miltenyi and J. Keller for the assistance with the MBE. This work was supported by the Belgian Inter-University Attraction Poles (IUAP) and Flemish Concerted Research Actions (GOA) programs, by the ESF "VORTEX" program and by the Fund for Scientific Research-Flanders (FWO). MJVB and KT are Postdoctoral Research Fellows of the FWO.

#### REFERENCES

- [1] HEBARD A. F., FIORY A. T. and SOMEKH S., *IEEE Trans. Magn.*, **1** (1977) 589.
- [2] BAERT M., METLUSHKO V. V., JONCKHEERE R., MOSHCHALOV V. V. and BRUYNSEAEDE Y., *Europhys. Lett.*, **29** (1995) 157.
- [3] BAERT M., METLUSHKO V. V., JONCKHEERE R., MOSHCHALOV V. V. and BRUYNSEAEDE Y., *Phys. Rev. Lett.*, **74** (1995) 3269.
- [4] MOSHCHALOV V. V., BAERT M., METLUSHKO V. V., ROSSEEL E., VAN BAELE M. J., TEMST K., JONCKHEERE R. and BRUYNSEAEDE Y., *Phys. Rev. B*, **54** (1996) 7385.
- [5] MOSHCHALOV V. V., BAERT M., METLUSHKO V. V., ROSSEEL E., VAN BAELE M. J., TEMST K., BRUYNSEAEDE Y. and JONCKHEERE R., *Phys. Rev. B*, **57** (1998) 1.
- [6] MARTÍN J. I., VÉLEZ M., NOGUÉS J. and SCHULLER I. K., *Phys. Rev. Lett.*, **79** (1997) 1929.
- [7] JACCARD Y., MARTÍN J. I., VÉLEZ M., VICENT J. L. and SCHULLER I. K., *Phys. Rev. B*, **58** (1998) 8232.
- [8] MARTÍN J. I., VÉLEZ M., HOFFMANN A., SCHULLER I. K. and VICENT J. L., *Phys. Rev. Lett.*, **83** (1999) 1022.
- [9] MORGAN D. J. and KETTERSON J. B., *Phys. Rev. Lett.*, **80** (1998) 3614.
- [10] VAN BAELE M. J., VAN LOOK L., TEMST K., LANGE M., BEKAERT J., MAY U., GÜNTHERODT G., MOSHCHALOV V. V. and BRUYNSEAEDE Y., *Physica C*, **332** (2000) 12.
- [11] VAN BAELE M. J., TEMST K., MOSHCHALOV V. V. and BRUYNSEAEDE Y., *Phys. Rev. B*, **59** (1999) 14674.
- [12] VAN BAELE M. J., BEKAERT J., TEMST K., VAN LOOK L., MOSHCHALOV V. V., BRUYNSEAEDE Y., HOWELLS G. D., GRIGORENKO A. N., BENDING S. J., BORGHIS G., *Phys. Rev. Lett.*, **86** (2001) 155.
- [13] LYUKSYUTOV I. F. and POKROVSKY V. L., *Phys. Rev. Lett.*, **81** (1998) 2344.
- [14] SASIK R. and HWA T., (unpublished), cond-mat/0003462.
- [15] ZEPER W. B., GREIDANUS F. J. A., CARCIA P. F. and FINCHER C. R., *J. Appl. Phys.*, **65** (1989) 4971.
- [16] LI Z. G. and CARCIA P. F., *J. Appl. Phys.*, **71** (1992) 842.
- [17] ZHONG Q., INNISS D., KJOLLER K. and ELINGS V. B., *Surf. Sci.*, **290** (1993) L688.
- [18] ALLENSPACH R., STAMPANONI M. and BISCHOF A., *Phys. Rev. Lett.*, **65** (1990) 3344.
- [19] MARMORKOS I. K., MATULIS A. and PEETERS F. M., *Phys. Rev. B*, **53** (1996) 2677.
- [20] JACKSON J. D., *Classical Electrodynamics - 3rd edition* (John Wiley & Sons, Inc., New York) 1999, p. 196.